

Non-activated transport of strongly interacting two-dimensional holes in GaAs

Jian Huang,¹ D. S. Novikov,¹ D. C. Tsui,¹ L. N. Pfeiffer,² and K. W. West²

¹*Department of Electrical Engineering, Princeton University, Princeton, New Jersey 08544, USA*

²*Bell Laboratories, Lucent Technologies, Murray Hill, New Jersey 07974, USA*

(Dated: December 2, 2024)

We report on the transport measurements of two-dimensional holes in GaAs field effect transistors with record low densities down to $7 \times 10^8 \text{ cm}^{-2}$. Remarkably, such a dilute system (with Fermi wavelength approaching $1 \mu\text{m}$) exhibits a non-activated conductivity that grows with temperature following a power law. We contrast it with the activated transport obtained from measuring more disordered samples, and discuss possible transport mechanisms in this strongly-interacting regime.

PACS numbers:

The question of how a strong Coulomb interaction can qualitatively alter an electronic system is fundamentally important. It has generated great interest in studying the transport in two-dimensional (2D) electron systems [1]. Since the interaction becomes effectively stronger with lower 2D electron density, samples with most dilute carriers are desirable to probe the interaction effects. As the density is lowered, strong enough disorder can localize the carriers so that the interaction effect is smeared by the insulating behavior. Therefore, a clean 2D environment is vital to uncover the underlying interaction phenomena.

For a long time, the dilute 2D carriers have been known as insulators characterized by activated conductivity. Specifically, in an Anderson insulator [2, 3], the conductivity follows the Arrhenius temperature dependence $\sigma \sim e^{-E_g/k_B T}$, where E_g is the mobility edge with respect to the Fermi level. The energy relaxation due to phonons in the impurity band results in a softer exponential dependence $\sigma \sim e^{-(T^*/T)^\nu}$, realized via the variable-range hopping (VRH) process [4, 5]. Here, the exponent $\nu = 1/3$ for non-interacting electrons [4], while $\nu = 1/2$ if the Coulomb gap opens up at the Fermi level [5]. Finally, strong Coulomb interactions are believed to crystallize the 2D system [6] which then can become pinned by arbitrarily small disorder. A relation $d\sigma/dT > 0$, being a natural consequence of the activated transport, eventually became a colloquial criterion of distinguishing an insulator from a metal [7].

The experimental results in the dilute carrier regime are known to be greatly influenced by the sample quality, which has much improved over time. The phonon-assisted hopping transport was observed in early experiments [7]. As the sample quality improved, the later experiments performed on 2D electrons in cleaner Si-MOSFETs demonstrated that the temperature-dependence of the resistivity $\rho = \sigma^{-1}$ can be either metal-like ($d\rho/dT > 0$), or insulator-like ($d\rho/dT < 0$), depending on whether the carrier density n is above or below a critical value n_c [8]. On the insulating side, where $n < n_c$, $\rho(T)$ grows exponentially with cooling [9]. Similar results have since been observed in various low

disorder 2D systems, and the resistivity on the insulating side has been consistently found to follow an activated pattern $\rho \sim e^{(T^*/T)^\nu}$, with ν varying between $1/3$ and 1 .

In this work, we focus on the transport properties of clean 2D holes in the dilute carrier regime where the insulating behavior is anticipated. To achieve high quality and low density, we adopt the GaAs/AlGaAs heterojunction insulated-gate field-effect transistor (HIGFET) where the carriers are only capacitively induced by a metal gate [10, 11, 12]. Because there is no intentional doping, the amount of disorder is likely to be less, and the nature of the disorder is different from that of the modulation doped samples. The transport of the 2D holes in such a HIGFET sample was observed to have a non-activated conductivity $\sigma(T)$ with almost linear temperature dependence for carrier densities as low as $1.5 \times 10^9 \text{ cm}^{-2}$ [13]. We have measured several high quality p-channel HIGFET samples (table I) with similar heterostructures as the one in Ref. [13]. The hole density p in our devices can be continuously tuned to as low as $7 \times 10^8 \text{ cm}^{-2}$, in which case the nominal Fermi wavelength $\lambda_F = (2\pi/p)^{1/2} \simeq 0.95 \mu\text{m}$.

Our main finding is that, even for the lowest density, the conductivity of the cleanest samples at base temperature is much larger than that of a typical insulator. Moreover, $\sigma(T)$ decreases with cooling in a non-activated fashion which is best approximated by a power-law $\sigma \propto T^\alpha$. The non-universal exponent α , $1 \lesssim \alpha \lesssim 2.2$, increases with decreasing density, and depends on the screening of the Coulomb interaction by the metal gate.

The device geometry is a standard $3 \text{ mm} \times 0.8 \text{ mm}$ Hall bar. The measurements were performed in a dilution refrigerator with a base temperature of 35 mK . At each value of the gate voltage, the mobility and density were

TABLE I: The samples and the corresponding barrier thicknesses d

Samples	alas4-2	11-17-001	11-15-002
Barrier	600nm	250nm	550nm

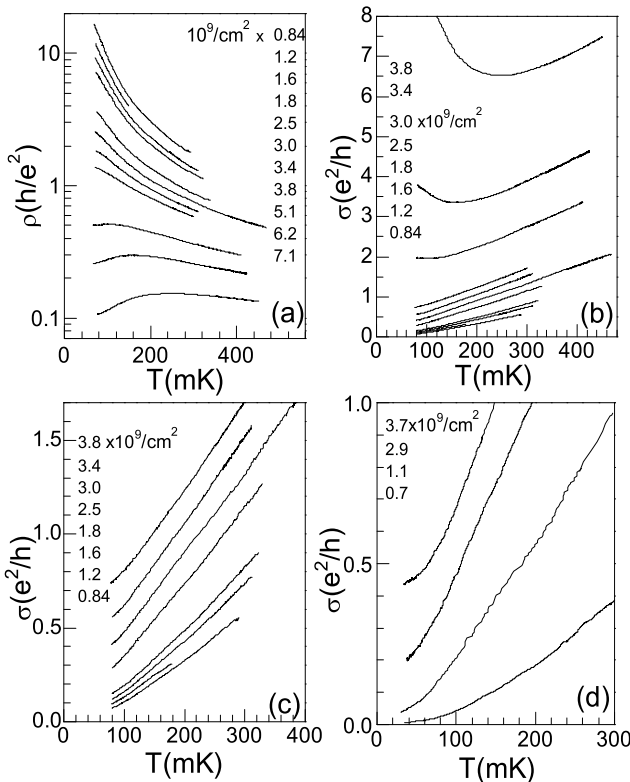


FIG. 1: Temperature dependence of (a) the resistivity and (b) the conductivity of sample alas4-2, for a set of specified hole densities. (c) The low-density curves from (b) magnified. (d) Conductivity from a similar clean sample 11-17-001.

determined through measuring the longitudinal resistivity ρ and its quantum oscillations in the magnetic field. The temperature dependence of the resistivity was measured with an ac four-terminal setup at high carrier density, while both ac and dc setups were used for the low-density high-impedance cases. To ensure linear response, current drive as small as 1 pA was used during the measurements at the lowest carrier density. Driving currents of different amplitudes were used for the low density cases and the measured resistivity did not change with varying the current drive.

The temperature dependence of the resistivity $\rho(T)$ for a number of hole densities from sample alas4-2 is shown in Fig. 1(a), with lowest temperature of 85 mK. At first glance, the density dependence of the $\rho(T)$ curves is similar to that found around the metal-to-insulator transition [7], with $p_c = 4 \times 10^9 \text{ cm}^{-2}$ being the critical density. For $p > p_c$, the system exhibits the apparent metallic behavior ($d\rho/dT > 0$) at sufficiently low temperatures. The downward bending of $\rho(T)$ becomes weaker as p approaches p_c , and disappears for lower p . The derivative $d\rho/dT$ then becomes negative, a conventional characteristic of an insulator [7], for the whole temperature range. At the transition, the resistivity is of the order of h/e^2 .

The value of p_c is very close to that obtained in a similar device in Ref. [12].

Fig. 1(b) shows the conductivities $\sigma(T)$ for the corresponding densities. For $1.8 \times 10^9 \text{ cm}^{-2} < p < 3.8 \times 10^9 \text{ cm}^{-2}$, the conductivity increases linearly with T at high temperatures (above ~ 200 mK). The linear regions are almost parallel for different densities, similar to that observed previously [12, 13]. For $p \leq 1.8 \times 10^9 \text{ cm}^{-2}$, $\sigma(T)$ deviates from the linear relation as described below. The linear dependence occurs at temperatures above the nominal Fermi temperature and will be studied in detail elsewhere [14].

Below we focus on the low-temperature conductivity $\sigma(T)$ for densities below the critical density $4 \times 10^9 \text{ cm}^{-2}$. These curves for the two cleanest samples are presented in Figs. 1(c) and (d), with the sample 11-17-001 cooled down to 35 mK. These curves are surprising in the following three aspects: (i) For densities from $2.5 \times 10^9 \text{ cm}^{-2}$ to $3.8 \times 10^9 \text{ cm}^{-2}$ in Fig. 1(c), the $\sigma(T)$ relations appear almost linear and parallel to each other. However, for the four lower densities, from $8 \times 10^8 \text{ cm}^{-2}$ to $1.8 \times 10^9 \text{ cm}^{-2}$, the conductivity deviates from the linear decrease at low temperatures; (ii) $\sigma(T)$ exhibits a slower change with T as the density is reduced, with weakest T -dependence close to the base temperature (note the linear scale in the plot); (iii) The conductivity values ($\sim 0.1e^2/h$) are considerably larger than those found in the more disordered sample which is described below.

We now contrast this anomalously slow decrease of $\sigma(T)$ in the "insulating" regime with the usual exponentially fast decrease of the conductivity observed in a more disordered sample 11-15-002 (Fig. 2). The sample mobility μ is much lower than those of the clean samples. For example, for $p = 1 \times 10^{10} \text{ cm}^{-2}$, $\mu \simeq 11,000 \text{ cm}^2/\text{Vs}$ for

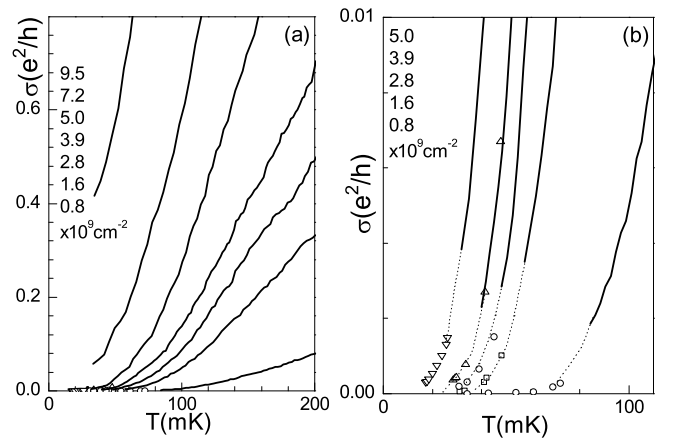


FIG. 2: (a) Activated conductivity of the more disordered sample 11-15-002. (b) Low-temperature zoom-in of (a). The solid curves and the scattered points are results from the ac and dc measurements for the same density, with the dotted lines being guides for the eye.

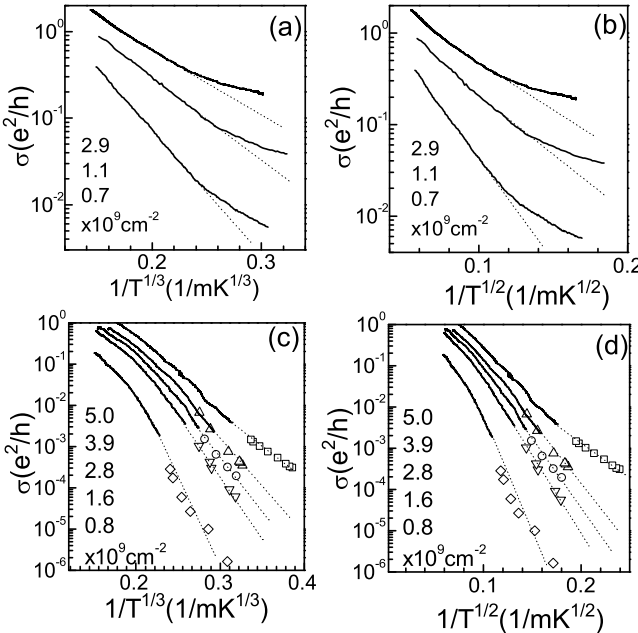


FIG. 3: Comparison of the conductivities $\sigma(T)$ with VRH transport models: (a), (c) Mott; (b), (d) Efros-Shklovskii. Panels (a) and (b) are results from the clean sample 11-17-001, and (c) and (d) are from the dirty sample 11-15-002. The solid curves and the scattered points are results from the ac and dc measurements respectively.

sample 11-15-002, and $\mu \simeq 850,000 \text{ cm}^2/\text{Vs}$ for sample 11-17-001. Also, the critical density $p_c \simeq 1 \times 10^{10} \text{ cm}^{-2}$ is much higher than the $p_c \simeq 3.5 \times 10^9 \text{ cm}^{-2}$ of sample 11-17-001. For the similar density range with that of the clean samples, the conductivities [Fig. 2(a)] for $p \leq 5 \times 10^9 \text{ cm}^{-2}$ collapse to zero at low temperatures. This is in clear contrast with the finite conductivities shown in Figs. 1(c) and (d) that are plotted on the same scale. The conductivity values are much lower than those in the cleanest samples. When zoomed in by a factor of 100 [Fig. 2 (b)], the conductivity shows a threshold behavior, absent in the cleanest samples, at characteristic temperatures that are density dependent. Note that the dc results (scattered points in the plot) match well with those from the ac measurements for the same densities.

In Fig. 3, we compare the measured conductivities with the VRH predictions according to Mott [4] and Efros-Shklovskii [5] for both the clean (11-17-001) and the more disordered (11-15-002) samples. The hopping conductivity $\sigma \sim e^{-(T^*/T)^\nu}$ is expected at low temperatures. However, in the clean sample, the conductivity [panels (a) and (b) in Fig. 3] is approximately linear (in the semi-log scale) at high temperatures but nonlinear at low temperatures. It clearly deviates from the VRH law (dotted lines) for both $\nu = 1/3$ and $\nu = 1/2$. Furthermore, the deviation increases with cooling indicating weaker than activated temperature dependence. On the other hand, the transport in the disordered sample [Fig. 3(c) and (d)]

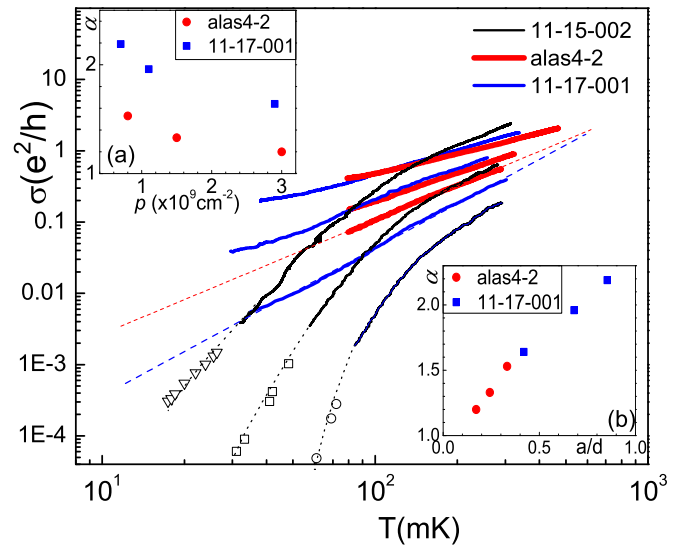


FIG. 4: Power-law $\sigma(T)$ behavior from clean samples, alas4-2 and 11-17-001, in comparison with the activated behavior in the more disordered sample 11-15-002. The densities p are $3.0, 1.8, 0.8 \times 10^9 \text{ cm}^{-2}$ for alas4-2; $2.9, 1.1, 0.7 \times 10^9 \text{ cm}^{-2}$ for 11-17-001; and $5.0, 2.8, 0.8 \times 10^9 \text{ cm}^{-2}$ for 11-15-002. Scattered symbols are the dc conductivity values for 11-15-002. Dashed lines are the power law fits $\sigma \propto T^\alpha$ for the two clean samples with the exponent α shown in the inset (a) as a function of density, and in inset (b) as a function of a/d , where $a = (\pi p)^{-1/2}$, and d is the distance to the gate.

fits the VRH models reasonably well for the lowest densities. The difference between $\nu = 1/2$ and $1/3$ is practically indistinguishable on a single decade of temperature range. From fitting to the $\nu = 1/3$ VRH law we estimate the localization length $\xi/a = \sqrt{27E_F/k_B T^*} \simeq 0.13$ in the units of the Wigner-Seitz radius $a = (\pi p)^{-1/2}$, with $T^* \approx 250 \text{ K}$ and $a \simeq 200 \text{ nm}$ for the lowest density $p = 8 \times 10^8 \text{ cm}^2$. The Coulomb-gap VRH fitting with $\nu = 1/2$ gives $T^* \approx 8.4 \text{ K}$, yielding $\xi \simeq 1 \mu\text{m}$. Although the estimates of ξ differ by a factor of 50, both are compatible with the localization of individual carriers.

The qualitative difference in the temperature dependence between the clean and the more disordered samples is also apparent in the log-log scale plot in Fig. 4 which contains the data from all three samples. The dependence $\log \sigma(\log T)$ for the two cleanest samples appears to be approximately linear, indicating a power-law-like relationship $\sigma \propto T^\alpha$. For each clean sample, the exponent α , which corresponds to the slope in the plot, increases with decreasing density. A comparison between the two cleanest samples reveals that α [found to be $1 \lesssim \alpha \lesssim 2.2$ as shown in the inset (a)] also depends on the sample structure (as discussed below). On the other hand, the conductivity for the more disordered sample 11-15-002 exhibits a clear downward bending, consistent with the activated behavior [Fig. 3 (c) and (d)]. Notice the low- T conductivity values in this sample are at least three or

ders of magnitude smaller than those in the clean ones.

The insulating character of our more disordered sample is consistent with previously observed insulators in lower quality 2D systems. However, our clean HIGFET results show that, with less disorder, the transport becomes non-activated, indicating the presence of delocalized states. As discussed below, the interaction is indeed crucial in this regime.

In HIGFETs, the metallic gate at distance d from the 2D hole layer (Table I) screens the $1/r$ interaction down to $1/r^3$ when $r \gtrsim 2d$. For the lowest densities, the interaction becomes effectively short-ranged, with the relevant parameter being the ratio a/d between the carrier spacing $\approx 2a$ and the screening radius $2d$. For our measurement, this ratio can be continuously varied in the range $0.1 < a/d < 0.85$. The effect of the screening is illustrated in the inset (b) of Fig. 4 where the power law exponent α from both clean samples is plotted as a function of a/d . The two samples have different barrier thickness d (Table I). Remarkably, $\alpha(a/d)$ from both samples fall onto a single curve indicating the important role played by the interaction. As discussed below, the interaction has different characteristics at short ($r \ll d$) and long ($r \gg d$) distances.

The short-distance $1/r$ -interaction is indeed very strong. If treated classically as a one-component plasma, the interaction parameter $\Gamma = E_C/k_B T \sim 100$, corresponding to an enormous Coulomb energy $E_C = e^2/\epsilon a \sim 10$ K, with $\epsilon = 13$. Since the temperature in our system is of the order of the Fermi energy, $E_F = \hbar^2/ma^2 \sim 100$ mK, quantum effects are important. A standard estimate of the strength of interaction is the quantum-mechanical parameter $r_s = a/a_B$, where $a_B = \hbar^2\epsilon/me^2$ is the Bohr radius. It requires the knowledge of the band mass m that has never been measured in such a dilute regime. Higher density cyclotron resonance measurements give $m \simeq 0.2 - 0.4m_e$ [15], whereas low-density theoretical estimates (based on the Luttinger parameters) [16] give $m \simeq 0.1m_e$. The r_s value for $p = 1 \times 10^9$ cm $^{-2}$ is in the range of 25 – 100 for the mass range of $m = 0.1m_e - 0.4m_e$.

The long-distance dipolar interaction is relatively weak for such low densities since the $1/r^3$ potential is short-ranged in two dimensions. Therefore, the liquid is favored over the Wigner crystal (WC) [17], as the quantum fluctuations ($\sim 1/r^2$) overcome the $1/r^3$ interaction. Meanwhile, even for a classical system, the 2D WC melting temperature $T_m \simeq E_C/130k_B$ is already low [18]: $T_m = 56$ mK for $p = 1 \times 10^9$ cm $^{-2}$. The screening further reduces T_m [19] to make the WC even harder to access. The absence of the pinned WC in our samples is corroborated by the non-activated transport in the linear response regime and the absence of singularity in $\sigma(T)$.

The above analysis shows that the interaction character is determined by the dimensionless screening parameter $\kappa = a/d$ (borrowed from plasma physics [19]), where

a and d can be independently controlled. For a fixed d , the interaction is effectively long-ranged for high densities ($a \ll d$) and short-ranged for low densities ($a \gg d$). By varying the density, one can continuously modify the state of the system. For sufficiently low densities ($a \gtrsim d$), a reentry into the Fermi-Liquid (FL) was suggested [20] based on its robustness to the short-range interactions. For larger densities, a sequence of mixed phases [21] was conjectured.

As for the transport, the disorder is also a crucial factor. For such low densities, the disorder potential variations at large length scale can easily exceed $E_F \sim 10$ μ V, so that the system can become separated into disconnected domains. The observed non-activated behavior indicates that the density is above the percolation threshold for our cleanest samples. In this case, the collective viscous flow of the electron liquid can be important to the transport. Particularly, in a FL, it leads to $\sigma \sim T^2$ [17, 22]. The observed exponent α (Fig. 4) increases from about 1 to 2 as the ratio a/d increases from 0.1 to 0.85. This tendency is in qualitative agreement with the FL reentry scenario.

In summary, we have observed a non-insulating behavior in the putatively insulating regime for hole densities down to 7×10^8 cm $^{-2}$. The conductivity strongly depends on the character of the electron interactions controlled by the density and the distance to the gate. These results suggest that the 2D holes form a strongly-correlated quantum liquid state with tunable properties.

This work has benefited from valuable discussions with Igor Aleiner, Boris Altshuler, Ravin Bhatt, and Mark Dykman. We also thank Stephen Chou for the use of his fabrication facilities. The work at Princeton University is supported by US DOE grant DEFG02-98ER45683, NSF grant DMR-0352533, and NSF MRSEC grant DMR-0213706.

- [1] T. Ando, A.B. Fowler, and F. Stern, Rev. Mod. Phys. **54**, 437 (1982).
- [2] P.W. Anderson, Phys. Rev. **109**, 1492 (1958).
- [3] E. Abrahams, P.W. Anderson, D.C. Licciardello, and T.V. Ramakrishnan, Phys. Rev. Lett. **42**, 673 (1979)
- [4] N.F. Mott, J. Non-Cryst. Solids **1**, 1 (1968).
- [5] B.I. Shklovskii and A.L. Efros, *Electronic Properties of Doped Semiconductors*, Springer-Verlag, Berlin (1984).
- [6] B. Tanatar and D. M. Ceperley, Phys. Rev. B **39**, 5005 (1989).
- [7] E. Abrahams, S.V. Kravchenko, and M.P. Sarachik, Rev. Mod. Phys. **73**, 251 (2001).
- [8] Kravchenko, S. V., G. V. Kravchenko, J. E. Furneaux, V. M. Pudalov, and M. D'Iorio, Phys. Rev. B **50**, 8039 (1994).
- [9] W. Mason, S. V. Kravchenko, G. E. Bowker, and J. E. Furneaux, 1995, Phys. Rev. B **52**, 7857
- [10] B. E. Kane, L. N. Pfeiffer, and K. W. West, Appl. Phys.

Lett. **67**, 1262 (1995).

[11] M. P. Lilly, J. L. Reno, J. A. Simmons, I. B. Spielman, J. P. Eisenstein, L. N. Pfeiffer, K. W. West, E. H. Hwang, and S. Das Sarma, Phys. Rev. Lett. **90**, 056806 (2003).

[12] Hwayong Noh, M. P. Lilly, D. C. Tsui, J. A. Simmons, L. N. Pfeiffer, and K. W. West, Phys. Rev. B **68**, 165308 (R) (2003).

[13] Hwayong Noh, M. P. Lilly, D. C. Tsui, J. A. Simmons, L. N. Pfeiffer, and K. W. West, Phys. Rev. B **68**, 241308 (R) (2003).

[14] Jian Huang *et al.* (unpublished).

[15] Pan W, Lai K, Bayrakci SP, Ong NP, Tsui DC, Pfeiffer LN, West KW, Appl. Phys. Lett. **83**, 3519 (2003).

[16] R. Winkler, *Spin-orbit coupling effects in two-dimensional electron and hole systems* (Springer, New York, 2003).

[17] B. Spivak, S. Kivelson, cond-mat/0510422 (2005).

[18] D.S. Fisher, B.I. Halperin, and R. Morf, Phys. Rev. B **20**, 4692 (1979).

[19] P. Hartmann, G.J. Kalman, Z. Donkó, and K. Kutasi, Phys. Rev. E **72**, 026409 (2005).

[20] B. Spivak and S. A. Kivelson Phys. Rev. B **70**, 155114 (2004).

[21] B. Spivak, Phys. Rev. B **67**, 125205 (2003).

[22] R. N. Gurzhi, Zh. Eksp. Teor. Fiz. **44**, 771 (1963) [Sov. Phys. JETP **17**, 521 (1963)]; Usp. Fiz. Nauk **94**, 689 (1968) [Sov. Phys. Usp. **11**, 255 (1968)]; R.N. Gurzhi, A.N. Kalinenko, and A.I. Kopeliovich, Phys. Rev. Lett. **74**, 3872 (1995).